

Universal Equation of State of Osmotic Pressure in Gelation Process

Takashi Yasuda,^{1,*} Naoyuki Sakumichi,^{1,†} Ung-il Chung,¹ and Takamasa Sakai^{1,‡}

¹*Department of Bioengineering, The University of Tokyo, 7-3-1 Hongo, Bunkyo-ku, Tokyo, Japan.*

(Dated: May 24, 2022)

The equation of state (EOS) of the osmotic pressure for linear-polymer solutions in good solvents is universally described by a scaling function. We experimentally measured the osmotic pressure of the gelation process via osmotic deswelling. It is found that the same scaling function for linear-polymer solutions also describes the EOS of the osmotic pressure throughout the gelation process, involving both sol and gel states. Furthermore, we reveal that the osmotic pressure of polymer gels is universally governed by the semidilute scaling law of linear-polymer solutions.

The statistical mechanics of groups of chains is the basis of polymer physics [1–4]. A remarkable example of this basis is the universality of linear-polymer solutions in good solvents [2, 5]. Their macroscopic collective properties are independent of the microscopic details of the system, because of the great length of polymer chains. This example of the universality of critical phenomena in the $O(n)$ -symmetric universality classes ($n = 1, 2, 3$ corresponding to the Ising, XY, and Heisenberg classes, respectively) is found in many systems, ranging from the fields of soft and hard condensed-matter physics to high-energy physics [6]. The above polymer solutions correspond to the limit of $n \rightarrow 0$ (self-avoiding walks) in three dimensions [2, 6], for which the critical exponent (the excluded volume parameter) $\nu \simeq 0.588$ can be computed by Monte Carlo simulations [7, 8], the ϵ expansion method [9], and the conformal bootstrap method [10, 11]. Furthermore, not only the critical exponents but also the asymptotic scaling functions themselves can be experimentally measured, such as the osmotic pressure [12, 13] and the correlation lengths of the density fluctuations [14].

Here, we focus on the equation of state (EOS) of osmotic pressure for linear-polymer solutions in good solvents, which is universally described by the scaling function [12, 13, 15–18]:

$$\hat{\Pi} = f(\hat{c}), \quad (1)$$

where $\hat{\Pi} \equiv \Pi M / (cRT)$ is the reduced osmotic pressure, and $\hat{c} \equiv c/c^*$ is the reduced polymer concentration normalized by the overlap concentration $c^* \equiv 1/(A_2 M)$. Here, M , R , T , and A_2 are the molar mass, gas constant, absolute temperature, and the second virial coefficient, respectively. The above definition of c^* is proportional [19] to the conventional definition of the overlap concentration $c_g^* \equiv 3M/(4\pi N_A R_g^3)$, at which the polymer chains begin to overlap each other to fill the space. Here, N_A and R_g are the Avogadro constant and the gyration radius of the polymer chain, respectively.

In the case of branched polymer solutions, it was reported that each EOS of regular star polymers with up to 18 arms exhibits only minor differences from the universal EOS (1) of linear polymers [13, 19–21]. Here, $\hat{c} \equiv c/c^*$ is the only universal scaling parameter (up to multiplication by a constant) [19]. In other words, c/c_g^* is not a universal scaling parameter because $c_g^*/c^* = 3\sqrt{\pi}\Psi^*$ includes the interpenetration factor Ψ^* , which is nonuniversal for a number of arms (e.g., $\Psi^* \simeq 0.24$ and 0.44 for linear and four-branched polymer solutions, respectively [22, 23]). Figure 1 demonstrates that the two kinds of linear polymer solution and four-branched polymer solutions converge to the single universal EOS (1). In the dilute regime ($c < c^*$), each molecular chain is sufficiently

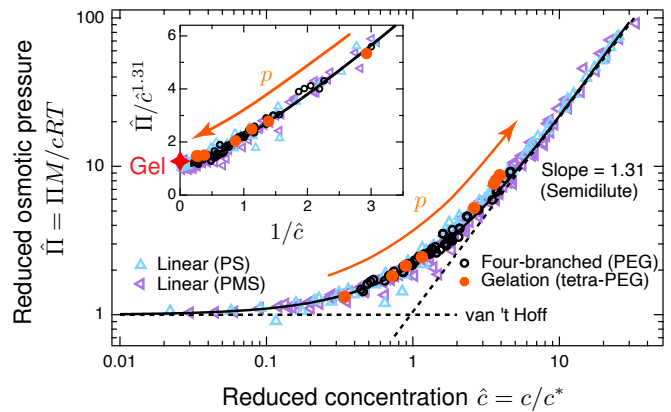


FIG. 1. Universal EOS of polymer solutions and gelation process in a good solvent. Main image shows the \hat{c} -dependence of $\hat{\Pi}$ in a log-log plot, and the inset shows the \hat{c}^{-1} -dependence of $\hat{\Pi}/c^{1.31}$. The triangles represent two kinds of linear polymer (poly(styrene) of $M = 51$ – 1900 kg/mol [13] and poly(α -methylstyrene) of $M = 70.8$ – 1820 kg/mol [12]) in toluene solutions. These converge to the universal EOS (1) (black solid curve), which is asymptotic to the van 't Hoff law ($\hat{\Pi} = 1$) as $\hat{c} \rightarrow 0$ and to the scaling law in Eq. (3) as $\hat{c} \rightarrow \infty$ (black dotted lines). The black circles represent four-branched polymer (poly(ethylene glycol)) solutions of $M = 10$ and 40 kg/mol. The orange filled circles represent the gelation process in sol states with various degrees of connectivity ($p = 0, 0.1, \dots, 0.5$) at a constant concentration ($c = 20$ g/L). The red star in the inset corresponds to the universal EOS for polymer gels.

* These authors contributed equally: T. Yasuda, N. Sakumichi

† Correspondence should be addressed to N. Sakumichi or T. Sakai: sakumichi@tetrapod.t.u-tokyo.ac.jp

‡ sakai@tetrapod.t.u-tokyo.ac.jp

isolated such that the universal EOS (1) is well described by the virial expansion [1]:

$$\hat{\Pi} = f(\hat{c}) = 1 + \hat{c} + \gamma \hat{c}^2 + \dots \quad (\text{for } 0 < \hat{c} < 1), \quad (2)$$

where $\gamma \simeq 0.25$ [1, 12] is the dimensionless virial ratio. In the semidilute regime ($c^* < c$), molecular chains become interpenetrated and the universal EOS (1) is asymptotic to the scaling law [2, 15]:

$$\hat{\Pi} = f(\hat{c}) \simeq K \hat{c}^{\frac{1}{3\nu-1}} \quad (\text{for } \hat{c} \gg 1), \quad (3)$$

where $K \simeq 1.1$ is the numerical constant and $1/(3\nu-1) \simeq 1.31$ if $\nu = 0.588$.

In the present study, we experimentally investigate the EOS of the osmotic pressure of polymer gels, including the whole gelation process. We measured the osmotic pressure in both the sol and gel states via osmotic deswelling in external polymer solutions [24–26]. Our findings are summarized in Fig. 1; the universality of EOS (1) holds for both the sol (orange filled circles) and gel (red star) states with only minor variations, although these systems are comprised of highly branched three-dimensional polymer networks. When gelation proceeds at a constant concentration c , the average molar mass M increases, and c^* decreases. Thus, both $\hat{\Pi}$ and \hat{c} continuously increase along the universal EOS (1) in the sol states. After the gelation (i.e., sol–gel transition), because polymer gels correspond to $M \rightarrow \infty$ and $c^* \rightarrow 0$, both $\hat{\Pi}$ and \hat{c} diverge to infinity in the gel states. According to the semidilute scaling law given by Eq. (3), $\hat{\Pi}/\hat{c}^{1.31}$ is always constant in gel states (red star in the inset of Fig. 1).

To statically reproduce the gelation process, we non-stoichiometrically tuned the mixing fractions s ($0 \leq s \leq 1/2$) of two kinds of precursor solution in an AB-type polymerization system (schematics in Fig. 2). Here, s is the molar fraction of the minor precursors to all precursors. We define the connectivity p ($0 \leq p \leq 1$) as the fraction of the reacted terminal functional groups, assuming reaction completion. By tuning s in accordance with $p = 2s$ [27, 28], we can obtain a desired p . Before gelation ($0 \leq p < p_{\text{gel}}$), polymer chains crosslink to form a polydisperse mixture of highly branched polymers with increases in the average molar mass M . After gelation ($p_{\text{gel}} \leq p \leq 1$), polymer networks crosslink to complete the reaction as the elasticity increases.

Based on our findings shown in Fig. 1, the “non-reduced” osmotic pressure Π during the gelation process is illustrated in Fig. 2. Unlike the sol states, the gel states have elastic contributions to the swelling pressure. According to Flory and Rehner [29], the total swelling pressure in the gel states (Π_{tot}) consists of two separate contributions as $\Pi_{\text{tot}} = \Pi_{\text{mix}} + \Pi_{\text{el}}$, where Π_{mix} and Π_{el} are the mixing and elastic contributions, respectively. We regard Π_{mix} as being the osmotic pressure in the gel states because Π_{mix} corresponds to the osmotic pressure in the sol state Π . As the connectivity p increases at a constant concentration c , the osmotic pressure Π in

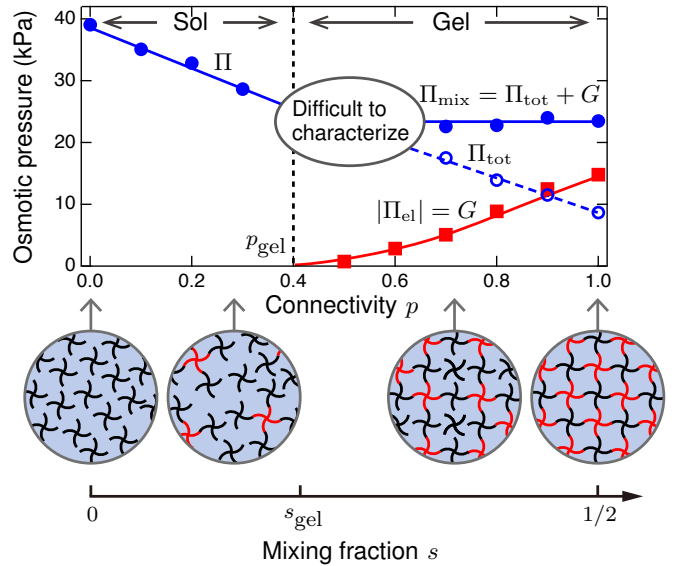


FIG. 2. Osmotic pressure during the gelation process at a constant polymer concentration ($c = 60 \text{ g/L}$) and a constant molar mass of precursors ($M = 10 \text{ kg/mol}$). By measuring Π_{tot} and G , we obtain $\Pi_{\text{mix}} = \Pi_{\text{tot}} + G$ in gel states. As the connectivity p increases, Π and Π_{tot} decrease, but Π_{mix} remains constant (blue curves). After gelation ($p_{\text{gel}} \leq p \leq 1$), the elasticity (red curve) increases. Here, p ($0 \leq p \leq 1$) is controlled by mixing two kinds of precursors non-stoichiometrically in an AB-type polymerization system. Gel samples with a low connectivity ($p_{\text{gel}} \leq p < 0.7$) were difficult to characterize, because of the outflow of small polymer clusters.

the sol states decreases, because the chemical reaction decreases the number density of the molecules. When the samples enter the gel states, the osmotic pressure Π_{mix} reaches a constant; polymer gels are always in a semidilute regime with an infinite molar mass.

Materials and Methods. — For a model system of AB-type polymerization in gelation, we used a tetra-PEG gel, synthesized by the AB-type cross-end coupling of two tetra-arm poly(ethylene glycol) (tetra-PEG) units of the same size [30]. Each end of the tetra-PEG is modified with mutually reactive maleimine (tetra-PEG MA) and thiol (tetra-PEG SH). We dissolved tetra-PEG MA and tetra-PEG SH (Nippon Oil & Fat Corporation) in a phosphate-citrate buffer with an ionic strength and pH of 200 mM and 3.8, respectively. For gelation, we mixed these solutions with equal molar masses M and equal concentrations c in various mixing fractions s . We held each sample in an enclosed space to maintain humid conditions at room temperature ($T \simeq 298 \text{ K}$) to allow the reaction to complete.

We prepared the four-branched polymer (precursor) solutions ($p = 0$) by dissolving tetra-PEG MA with molar masses of $M = 10$ and 40 kg/mol and initial concentrations $c_0 = 20\text{--}120 \text{ g/L}$. Herein, we define the polymer concentration (c_0 and c) as the precursor weight divided

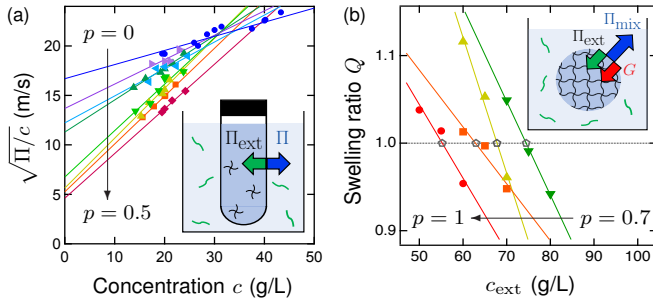


FIG. 3. Osmotic deswelling in external polymer solutions to measure Π and Π_{mix} in (a) sol and (b) gel samples, respectively. For each plot, precursors are $M = 10 \text{ kg/mol}$. Each line is the least squares fit to the data for each p . (a) Square root plots of Π of sol samples on $c_0 = 20 \text{ g/L}$ for the degrees of connectivity $p = 0, 0.1, 0.2, 0.25, 0.3, 0.35, 0.4, 0.5$. We immersed samples with a micro-dialyzer in external polymer (PVP) solutions. We can determine Π , because $\Pi = \Pi_{\text{ext}}$ at equilibrium. (b) Swelling ratio Q of gel samples on $c_0 = 60 \text{ g/L}$ for $p = 0.7, 0.8, 0.9, 1$ in equilibrium state in external polymer (PVP) solutions. We directly immersed samples in the external solutions of various concentrations c_{ext} . We can determine Π_{mix} , because $\Pi_{\text{mix}} = \Pi_{\text{ext}} + G$ at equilibrium.

by the solvent volume, rather than the solution volume, to extend the universality of the EOS (1) to higher concentrations (see Supplemental Material, Sec. S1). We prepared the sol and gel samples in the gelation process, dissolving precursors with $M = 10 \text{ kg/mol}$. For $c_0 = 20 \text{ g/L}$, we set $p = 2s = 0.1, 0.2, 0.25, 0.3, 0.35, 0.4, 0.5$ (sol samples). For $c_0 = 40, 60, 80, 120 \text{ g/L}$, we set $p = 2s = 0.1, 0.2, 0.3$ (sol samples) and $0.7, 0.8, 0.9, 1$ (gel samples). Sec. S2 of Supplemental Material describes the determination of these measurement ranges.

We measured the osmotic pressures of the sol states Π , using controlled aqueous poly(vinylpyrrolidone) (PVP, K90, Sigma Aldrich) solutions whose concentration dependence of osmotic pressure Π_{ext} was measured by Vink [31] (Supplemental Material, Sec. S3). As shown in the schematic in Fig. 3(a), each solution sample was placed in a micro-dialyzer (MD300, Scienova), which had a semipermeable membrane with a mesh size of 3.5 kDa. We immersed each dialyzer in aqueous polymer (PVP) solutions at a certain concentration c_{ext} with stirring. This system achieved equilibrium at $\Pi = \Pi_{\text{ext}}$. (Achievement of swelling equilibrium was assured as described in Sec. S4 of Supplemental Material.) At that time, each solution sample was changed in weight and concentration from its initial to equilibrium states as $w_0 \rightarrow w$ and $c_0 \rightarrow c$, respectively. Assuming a constant weight density and small deformation for the sample, we obtained the concentration at equilibrium as $c = c_0/Q$, where $Q = w/w_0$ is the swelling ratio. In examining the gelation process (orange filled circles in Fig. 1 and Fig. 2), we compared Π of the “as-prepared” sol samples at equal concentrations $c = c_0$ with various values of p . We determined Π of each as-prepared sol sample by measuring the swelling ratio Q as a linear function of c_{ext} . (The

method used to determine Π of the as-prepared samples is the same as that used for gels, as detailed below.)

To evaluate the parameters M and c^* from $\Pi = \Pi(c)$ measured at each p , we used the square root plots [1], as shown in Fig. 3(a). From the virial expansion (2), we have $\hat{\Pi} = [1 + \hat{c}/2 + (\gamma - 1/4) \hat{c}^2/2]^2 + O(\hat{c}^3)$. Together with $\gamma \simeq 1/4$ (Supplemental Material, Sec. S5) for certain solutions of few-branched polymers, we have $\sqrt{\Pi/c} \simeq \sqrt{RT/M} [1 + c/(2c^*)]$ for small c/c^* . Thus, the intercepts and slopes of each fitting line in Fig. 3(a) give M and c^* , respectively, for each p . The obtained M and c^* values are consistent with the scaling prediction of $c^* \sim M^{1/(3\nu-1)}$ with $\nu = 0.588$ (Supplemental Material, Sec. S6).

We measured the osmotic pressure in the as-prepared gel states Π_{mix} via the osmotic deswelling. As shown in the schematic in Fig. 3(b), we immersed each gel sample directly in the external aqueous polymer (PVP) solutions with various concentrations c_{ext} , because the surfaces of the gels function as semipermeable membranes. Then, each gel sample swells or deswells from the as-prepared state to the equilibrium state as $\Pi_{\text{mix}} + \Pi_{\text{el}} = \Pi_{\text{ext}}$, changing its weight and concentration from the initial to equilibrium states as $w_0 \rightarrow w$ and $c_0 \rightarrow c$, respectively. The swelling ratio $Q = w/w_0$ was measured and interpolated as a linear function of c_{ext} for each gel sample (e.g., the samples of various connectivity p at $c_0 = 60 \text{ g/L}$, as given in Fig. 3(b)). By using the c_{ext} -dependence of Q , we evaluated c_{ext} and Π_{ext} such that each gel sample maintained its weight ($Q = 1$) and concentration ($c = c_0$). We assumed that $\Pi_{\text{el}} = -G$ [32] and evaluated $\Pi_{\text{mix}} = \Pi_{\text{ext}} + G$ of each as-prepared gel sample, where G is the shear modulus as measured by rheometry (Supplemental Material, Sec. S7).

Results and Analysis. — The main panel in Fig. 4(a) shows the c -dependence of the osmotic pressure in the unreacted four-branched polymer solutions ($p = 0$) and in the reaction-completed polymer gels ($p = 1$). In the wide concentration range c , the experimental results of the former and latter are in remarkably good agreement with the universal EOS (1) for linear polymer solutions and with the semidilute scaling law $\Pi \propto c^{3\nu/(3\nu-1)}$, respectively. With the increase in c , Π in polymer solutions (black curve) is asymptotic to Π_{mix} in polymer gels (red line). This asymptotic relationship suggests that the Π_{mix} of polymer gels is governed by the semidilute scaling law in Eq. (3) with $K \simeq 1.1$ for polymer solutions.

The inset in Fig. 4(a) shows the p -dependence of Π and Π_{mix} throughout the gelation process ($0 \leq p \leq 1$). In the sol states ($0 \leq p < p_{\text{gel}}$), Π decreases as p increases, because the average molar mass M increases. As c increases, the extent of the decrease in the osmotic pressure itself decreases. In particular, for $c = 120 \text{ g/L}$, Π and Π_{mix} are constant throughout the gelation process ($0 \leq p \leq 1$), because the precursor solution is in the semidilute regime even at $p = 0$. In the gel states ($p_{\text{gel}} < p \leq 1$), Π_{mix} is constant even if p increases. In

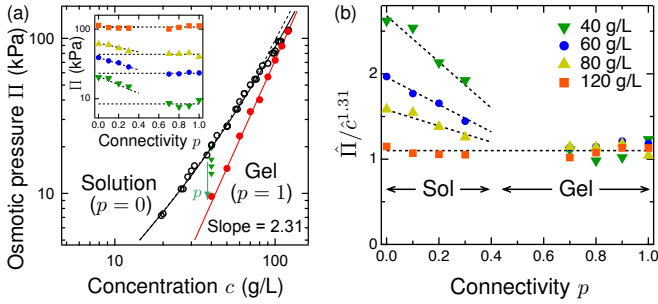


FIG. 4. Osmotic pressure during the gelation process. The molar mass of precursors is $M = 10$ kg/mol, corresponding to the overlap concentration $c^* \simeq 58$ g/L at $p = 0$. (a) Osmotic pressure in the unreacted four-branched polymer solutions (black circles) and in the reaction-completed polymer gels (red filled circles). The former and latter are in very good agreement with the universal EOS (1) (black curve) and with the semidilute scaling law $\Pi \propto c^{2.31}$ (red line), respectively. Here, $3\nu/(3\nu - 1) \simeq 2.31$ for $\nu \simeq 0.588$. The black dotted curve is the virial expansion (2) up to the third-order terms. As p increases (green triangles), Π decreases in sol states ($0 \leq p < p_{\text{gel}}$) and becomes constant in gel states ($p_{\text{gel}} < p \leq 1$). The inset shows the osmotic pressure during the gelation process at a constant polymer concentration $c = c_0 = 40, 60, 80, 120$ g/L. The green triangles ($c = 40$ g/L) are the same as those in the main panel. The blue circles ($c = 60$ g/L) are used in Fig. 2. (b) Connectivity (p) dependence of $\hat{\Pi}/\hat{c}^{1.31}$. The symbols and data are the same as those in the inset of (a). In gel states, $\hat{\Pi}/\hat{c}^{1.31}$ converge to the universal value 1.1, which is independent of p and c .

general, the osmotic pressure is dependent and independent of the average molar mass in the dilute and semidilute regimes, respectively [2]. Thus, the constant Π_{mix} in the gel states ($p_{\text{gel}} < p \leq 1$) indicates that polymer gels are always in the semidilute regime, because of the infinite molar mass of the polymer networks.

We can interpret Π during the gelation process in the sol states ($0 \leq p < p_{\text{gel}}$) in terms of the universal EOS (1). By using M and c^* evaluated in Fig. 3(a) at each p , we changed the state variables (from c and Π to \hat{c} and $\hat{\Pi}$), yielding the orange filled circles in Fig. 1. Remarkably, the gelation process in sol states ($p = 0, 0.1, \dots, 0.5$) obeys the universal EOS (1), although these systems continue to form multi-branched polymer clusters. Considering this in tandem with the semidilute scaling law observed in the gel states ($\Pi_{\text{mix}} \propto c^{2.31}$), it is expected that $\hat{\Pi}_{\text{mix}}$ in the gel states ($p_{\text{gel}} < p \leq 1$) will conform to the semidilute scaling law given by Eq. (3) of linear-polymer solutions (red line in Fig. 4(a)) with $K \simeq 1.1$.

Based on the above expectation, we propose a universal EOS of osmotic pressure Π_{mix} for polymer gels as

$$K = \frac{\hat{\Pi}_{\text{mix}}}{\hat{c}^{1/(3\nu-1)}} \equiv \frac{Mc^{*1/(3\nu-1)}\Pi_{\text{mix}}}{RTc^{3\nu/(3\nu-1)}}, \quad (4)$$

where $K \simeq 1.1$. We note that $\hat{\Pi}_{\text{mix}}/\hat{c}^{1/(3\nu-1)}$ is finite, al-

though both $\hat{c} \equiv c/c^*$ and $\hat{\Pi}_{\text{mix}} \equiv \Pi_{\text{mix}}M/(cRT)$ diverge to infinity, because gels correspond to infinite molar mass $M \rightarrow \infty$ and $c^* \rightarrow 0$. In Fig. 4(b), we demonstrate that $\hat{\Pi}_{\text{mix}}/\hat{c}^{1/(3\nu-1)}$ converge to the universal value $K \simeq 1.1$, which is independent of p and c , after the gelation ($p_{\text{gel}} \leq p \leq 1$). Thus, in the inset of Fig. 1, the gel states are positioned at $(1/\hat{c}, \hat{\Pi}_{\text{mix}}/\hat{c}^{1.31}) \simeq (0, 1.1)$ (red star). We obtained Fig. 4(b) by setting a constant value for $Mc^{*1/(3\nu-1)}$ and substituting Π and Π_{mix} (shown in the inset of Fig. 4(a)) into Eqs. (3) and (4), respectively. (Further details are given in Sec. S6 of Supplemental Material.) This procedure demonstrates that we can determine Π_{mix} for any polymer gel by measuring a non-universal parameter $Mc^{*1/(3\nu-1)}$.

Concluding remarks. — We have experimentally measured the osmotic pressure of polymer gels throughout the gelation process. We find that the universal EOS (1) of the osmotic pressure for linear-polymer solutions describes the osmotic pressure throughout the gelation process involving both the sol and gel states (Fig. 1). In the sol states, both $\hat{\Pi}$ and \hat{c} continuously increase according to the universal EOS (1) with an increase in the average molar mass (orange filled circles in Fig. 1). In the gel states, the osmotic pressure of polymer gels is universally governed by the semidilute scaling law (4) (red star in Fig. 1 and Fig. 4(b)). Here, both $\hat{\Pi}$ and \hat{c} diverge to infinity, because the gel states correspond to the average molar mass $M \rightarrow \infty$ and the overlap concentration $c^* \rightarrow 0$. In addition, we have demonstrated that Eq. (4) enables the determination of Π_{mix} for any polymer gel by measuring a non-universal parameter $Mc^{*1/(3\nu-1)}$.

Because polymer gels are open systems that can swell and deswell by exchanging solvents with the human body, an understanding of the osmotic pressure is essential for controlling the swelling of polymer gels. Our findings are not only conceptually important to polymer physics, but also practically useful, encouraging biomedical applications of polymer gels such as soft contact lenses, adhesion barriers, sealants, and artificial vitreous humor.

ACKNOWLEDGMENTS

We thank Masao Doi, Yuichi Masubuchi, Takashi Ueyama, and Xiang Li for their useful comments. This work was supported by the Japan Society for the Promotion of Science (JSPS) through the Grants-in-Aid for Early Career Scientists grant number 19K14672 to N.S., Scientific Research (B) grant number 18H02027 to T.S., and Scientific Research (S) grant number 16H06312 to U.C. This work was also supported by the Japan Science and Technology Agency (JST) CREST grant number JP-MJCR1992 to T.S. and COI grant number JPMJCE1304 to U.C.

[1] P. J. Flory, *Principles of Polymer Chemistry* (Cornell University Press, Ithaca, 1953).

[2] P. G. de Gennes, *Scaling Concepts in Polymer Physics* (Cornell University Press, Ithaca, 1979).

[3] I. M. Lifshitz, A. Y. Grosberg, and A. R. Khokhlov, *Rev. Mod. Phys.* **50**, 683 (1978).

[4] S. Panyukov, and Y. Rabin, *Phys. Rep.* **269**, 1 (1996).

[5] Y. Oono, *Adv. Chem. Phys.* **61**, 301 (1985).

[6] A. Pelissetto, and E. Vicari, *Phys. Rep.* **368**, 549 (2002).

[7] N. Clisby, *Phys. Rev. Lett.* **104**, 055702 (2010).

[8] N. Clisby, and B. Dünweg, *Phys. Rev. E* **94**, 052102 (2016).

[9] M. V. Kompaniets, and E. Panzer, *Phys. Rev. D* **96**, 036016 (2017).

[10] H. Shimada, and S. Hikami, *J. Stat. Phys.* **165**, 1006 (2016).

[11] S. Hikami, *Prog. Theor. Exp. Phys.* **2018**, 123I01 (2018).

[12] I. Noda, N. Kato, T. Kitano, and M. Nagasawa, *Macromolecules* **14**, 668 (1981).

[13] Y. Higo, N. Ueno, and I. Noda, *Polym. J.* **15**, 367 (1983).

[14] P. Wiltzius, H. R. Haller, D. S. Cannell, and D. W. Schaeffer, *Phys. Rev. Lett.* **51**, 1183 (1983).

[15] J. Des Cloizeaux, *J. Phys. (Paris)* **36**, 281 (1975).

[16] J. Des Cloizeaux, and I. Noda, *Macromolecules* **15**, 1505 (1982).

[17] T. Ohta, and Y. Oono, *Phys. Lett.* **89A**, 460 (1982).

[18] T. Ohta, and A. Nakanishi, *J. Phys. A: Math. Gen.* **16**, 4155 (1983).

[19] W. Burchard, *Adv. Polym. Sci.* **143**, 113 (1999).

[20] M. Adam, L. J. Fetters, W. W. Graessley, and T. A. Witten, *Macromolecules* **24**, 2434 (1991).

[21] G. Merkle, W. Burchard, P. Lutz, K. F. Freed, and J. Gao, *Macromolecules* **26**, 2736 (1996).

[22] A. M. Rubio, and J. J. Freire, *Macromolecules* **29**, 6946 (1996).

[23] M. Okumoto, Y. Nakamura, T. Norisuye, and A. Teramoto, *Macromolecules* **31**, 1615 (1998).

[24] J. Bastide, S. Candau, and L. Leibler, *Macromolecules* **14**, 719 (1981).

[25] F. Horkay, and M. Zrinyi, *J. Macromol. Sci., Part B: Phys.* **25**, 307 (1986).

[26] F. Horkay, I. Tasaki, and P. J. Basser, *Biomacromolecules* **1**, 84 (2000).

[27] T. Sakai, T. Katashima, T. Matsushita, and U. I. Chung, *Polym. J.* **48**, 629 (2016).

[28] Y. Yoshikawa, N. Sakumichi, U. I. Chung, and T. Sakai, *Soft Matter* **15**, 5017 (2019).

[29] P. J. Flory, and J. Rehner, *J. Chem. Phys.* **11**, 521 (1943).

[30] T. Sakai, T. Matsunaga, Y. Yamamoto, C. Ito, R. Yoshida, S. Suzuki, N. Sasaki, M. Shibayama, and U. I. Chung, *Macromolecules* **41**, 5379 (2008).

[31] H. Vink, *Eur. Polym. J.* **7**, 1411 (1971).

[32] H. M. James, and E. Guth, *J. Polym. Sci.* **4**, 153 (1949).

Supplemental Material for:
“Universal Equation of State of Osmotic Pressure in Gelation Process”

Takashi Yasuda,^{1,*} Naoyuki Sakumichi,^{1,†} Ung-il Chung,¹ and Takamasa Sakai^{1,‡}

¹Department of Bioengineering, The University of Tokyo, 7-3-1 Hongo, Bunkyo-ku, Tokyo, Japan.

(Dated: May 24, 2022)

S1. DEFINITION OF POLYMER CONCENTRATION

In the main text, we adopted a different definition of the polymer concentration (c_0 and c) than that used conventionally (\tilde{c}_0 and \tilde{c}) in order to extend the universality of the EOS of osmotic pressure to higher concentrations. In this section, we demonstrate the applicability of the above claim by comparing the EOSs determined using each of the definitions. The conventional polymer concentration is defined by

$$\tilde{c} = \frac{W_{\text{polymer}}}{V_{\text{solution}}}, \quad (\text{S1})$$

where W_{polymer} and V_{solution} are the polymer weight and solution volume, respectively. We note that V_{solution} includes not only the solvent volume V_{solvent} , but also the polymer volume V_{polymer} as $V_{\text{solution}} \simeq V_{\text{solvent}} + V_{\text{polymer}}$. For the EOS to be universal, the polymer chains must be excessively thin and their volume negligibly small [S1]; the universality is affected by V_{polymer} as the polymer concentration increases. Thus, we adopt the following definition:

$$c = \frac{W_{\text{polymer}}}{V_{\text{solvent}}}. \quad (\text{S2})$$

This definition in Eq. (S2) is similar to the consideration of the volume of a molecule in the van der Waals EOS for a real gas. In other words, the extent of polymer chain motion is considered as V_{solvent} , which is the total solution volume V_{solution} minus its own volume V_{polymer} . Figure S1 compares the two EOSs determined using these definitions in Eqs. (S1) and (S2) for the two linear polymer solutions of (a) poly(α -methylstyrene) (PMS) [S2] and (b) poly(styrene) (PS) [S3]. Adopting the definition given by Eq. (S1), the scaling slopes in the semidilute regime are 1.37 and 1.47 in the PMS and PS solutions, respectively. These slopes are larger than the theoretical prediction $1/(3\nu - 1) \simeq 1.31$ for a good solvent ($\nu \simeq 0.588$) [S1] because of the influence of the polymer volume at high concentrations. Adopting the definition in Eq. (S2), however, the scaling slopes in the

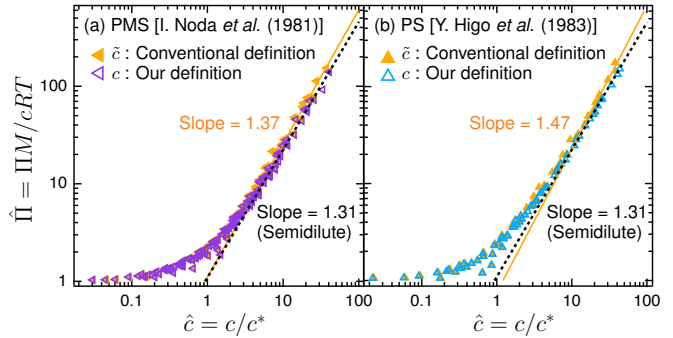


FIG. S1. Comparison of EOSs using the different definitions of polymer concentration given in Eqs. (S1) and (S2) for (a) poly(α -methylstyrene) [S2] and (b) poly(styrene) [S3] in toluene solutions. We use \tilde{c} and c to plot the filled and unfilled triangles, respectively. In the semidilute regime ($c^* < c$), the universal EOS is asymptotic to the scaling law [S1] as $\hat{\Pi} \propto \hat{c}^{1/(3\nu-1)}$ (Eq. (3) in the main text), where $1/(3\nu-1) \simeq 1.31$ for a good solvent ($\nu \simeq 0.588$).

semidilute regime for both the PMS and PS solutions asymptotically approach the theoretical prediction 1.31 as c increases. This emphasizes the universality of polymer solutions in higher concentrations in adopting the concentration definition in Eq. (S2). In the main text, therefore, we adopted Eq. (S2) as the polymer concentration and analyzed the universal scaling function.

S2. LIMITATIONS OF THE MEASUREMENT OF OSMOTIC PRESSURE

In the experiment, there are several limitations to the measurement of osmotic pressure via osmotic deswelling. Precursor-solution samples ($p = 0$) of higher concentrations ($c_0 > 120$ g/L) were excluded from the measurement due to our limited knowledge of the external polymer (PVP) solutions Π_{ext} . Sol samples ($0 \leq p < p_{\text{gel}}$) near their gelation points p_{gel} could not be measured due to viscosity divergences. Gel samples with a low connectivity ($p_{\text{gel}} < p < 0.7$) were difficult to characterize for the following two reasons: gels lost their shapes and weights because of their low elasticity, and we cannot uniquely determine the equilibrium state in the present osmotic pressure measurement because of the outflow of small polymer clusters. Gel samples ($p = 1$) at low concentrations ($c_0 < 40$ g/L) were excluded from our analysis because these samples became heterogeneous as a

* These authors contributed equally: T. Yasuda, N. Sakumichi

[†] Correspondence should be addressed to N. Sakumichi or T. Sakai: sakumichi@tetrapod.t.u-tokyo.ac.jp

‡ sakai@tetrapod.t.u-tokyo.ac.jp

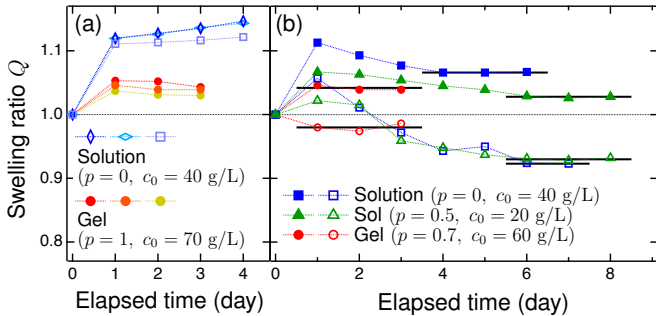


FIG. S2. Time courses of swelling ratio Q in swelling experiments (see Fig. 3 in the main text). We use solution ($p = 0$), sol ($0 < p < p_{\text{gel}}$), and gel ($p \geq p_{\text{gel}}$) samples whose precursors are $M = 10$ kg/mol. (a) Reproducibility of Q for the solution and gel samples in external polymer (PVP) solutions on $c_{\text{ext}} = 70$ g/L. For each sample, three representative experiments are in good agreement with each other, indicating high reproducibility. (b) Relaxation to swelling equilibrium states. For solution samples, we set $c_{\text{ext}} = 75$ g/L (blue filled squares) and $c_{\text{ext}} = 85$ g/L (blue open squares). For sol samples, we set $c_{\text{ext}} = 35$ g/L (green filled triangles) and $c_{\text{ext}} = 40$ g/L (green open triangles). For gel samples, we set $c_{\text{ext}} = 70$ g/L (red filled circles) and $c_{\text{ext}} = 75$ g/L (red open circles).

result of phase separation.

S3. OSMOTIC PRESSURE OF PVP SOLUTIONS

In the main text, we measured the osmotic pressure of samples by using the controlled aqueous poly(vinylpyrrolidone) (PVP) solutions. According to Vink [S4], the osmotic pressure Π_{ext} of an aqueous PVP solution is given by

$$\Pi_{\text{ext}} = 21.27c_{\text{ext}} + 1.63c_{\text{ext}}^2 + 0.0166c_{\text{ext}}^3, \quad (\text{S3})$$

for the PVP concentration $c_{\text{ext}} \leq 200$ g/L. Equation (S3) was precisely determined by using an osmometer with an organic liquid manometer, mercury manometer, and manostat. We note that c_{ext} in Eq. (S3) is defined as the polymer weight divided by the solution volume, i.e., Eq. (S1), which differs from the definition of the polymer concentration (c and c_0) used in the main text, i.e., Eq. (S2) (see Supplementary Sec. S1).

S4. ACHIEVEMENT OF SWELLING EQUILIBRIUM

To confirm the reproducibility of the swelling experiment described in the main text, we show the swelling ratio Q as a function of the elapsed time for solution ($p = 0$) and gel ($p = 1$) samples in Fig. S2(a). We immersed each sample (with or without the micro-dialyzer) in external polymer (PVP) solutions at a certain concentration c_{ext} (see Fig. 3 in the main text). Each sample

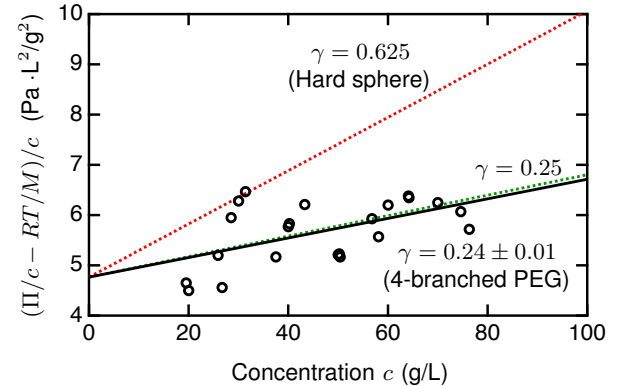


FIG. S3. Concentration dependence of $(\Pi/c - RT/M)/c$ for four-branched polymer (PEG) solutions (black circles) with $M = 8.8(1)$ kg/mol and $c^* = 58.5(4)$ g/L. Here, the values in parentheses represent the standard error estimated from the blue circles and line ($p = 0$) in Fig. 3(a) in the main text. We obtained the black line from a least-squares fit. According to Eq. (S4), the black line gives γ of four-branched polymer (PEG) solutions as $\gamma = 0.24(1)$. For comparison, we show the slopes corresponding to $\gamma = 0.25$ for linear polymer solutions [S5] and $\gamma = 0.625$ for hard spheres [S6].

changes in weight ($w_0 \rightarrow w$) and concentration ($c_0 \rightarrow c$) from the initial to equilibrium states. We determined the swelling ratio as $Q = w/w_0$.

To ensure that each sample achieved the equilibrium state in the swelling experiment, we show the relaxation processes for solutions ($p = 0$), sol ($0 < p < p_{\text{gel}}$), and gel ($p_{\text{gel}} < p \leq 1$) samples in Fig. S2(b). For each sample, we achieved both the swelling (filled symbols) and deswelling (unfilled symbols) conditions by adjusting the concentration of the external solutions c_{ext} . To achieve swelling equilibrium states (horizontal black lines), one week was needed for the solution and sol samples and a few days were needed for the gel samples. Here, we determined the swelling equilibrium as the point at which the swelling ratio Q remained constant for three days.

S5. THIRD VIRIAL COEFFICIENT OF FOUR-BRANCHED POLYMER SOLUTION

We evaluated the third virial coefficient from the c -dependence of Π in a four-branched polymer (PEG) solution (i.e., the precursor solutions ($p = 0$) in Fig. 4(a) in the main text). In terms of the universal EOS, the third virial coefficient corresponds to the dimensionless virial ratio γ defined in Eq. (2) in the main text. From the virial expansion up to the third terms (Eq. (2) in the main text), we have

$$\left(\frac{\Pi}{c} - \frac{RT}{M} \right) \frac{1}{c} = \frac{RT}{Mc^*} \left(1 + \frac{c\gamma}{c^*} \right). \quad (\text{S4})$$

In Fig. 3(a) in the main text, we obtain $M = 8.9(1)$ kg/mol and $c^* = 58.5(4)$ g/L at $T = 298$ K, where the

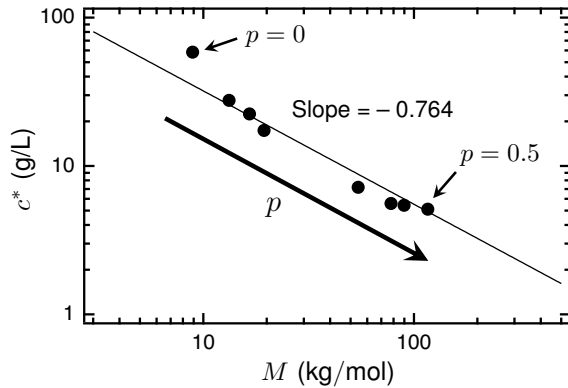


FIG. S4. Relationship between the overlap concentration c^* and the number average molar mass M during the gelation process in sol states ($0 \leq p < p_{\text{gel}}$). This result agrees with the scaling prediction in Eq. (S5) with $1 - 3\nu \simeq -0.764$ for a good solvent ($\nu \simeq 0.588$).

values in parentheses represent the standard error. Thus, the c -dependence of $(\Pi/c - RT/M)/c$ gives γ of four-branched polymer (PEG) solutions, as shown in Fig. S3. This analysis gave $\gamma = 0.24(1)$, which is consistent with $\gamma \simeq 0.25$ for linear polymer solutions [S5] within the error bounds. The consistency of γ between linear and four-branched polymer solutions indicates that the effect of a small number of branching on osmotic pressure is negligibly small in terms of the universal EOS.

S6. M AND c^* DURING THE GELATION PROCESS

We experimentally determined the average molar mass M and the overlap concentration c^* during the gelation process to obtain the universal scaling parameters \hat{c} and $\hat{\Pi}$ in Figs. 1 and 4(b) in the main text. When gelation proceeds at a constant concentration c_0 , M increases and the corresponding c^* decreases. Assuming the scaling relation of gyration radius R_g to be $\langle R_g^2 \rangle \propto M^{2\nu}$ [S1], we have

$$c^* \equiv \frac{M}{4\pi^{\frac{3}{2}} \langle R_g^2 \rangle^{\frac{3}{2}} N_A \Psi^*} \propto M^{1-3\nu}, \quad (\text{S5})$$

during the gelation process ($0 \leq p \leq 1$) if the interpenetration factor Ψ^* is constant as p increases.

To confirm M and c^* in the sol states ($0 \leq p < p_{\text{gel}}$) for $c_0 = 20 \text{ g/L}$, which were experimentally obtained in Fig. 3(a) in the main text, we compare the results with the corresponding scaling law of Eq. (S5). Each M and c^* was used to yield the orange filled circles in Fig. (1) in the main text. Figure S4 shows that the obtained M and c^* in the sol states (black circles) were consistent with the scaling prediction (black line) of Eq. (S5). Here, the deviation at $p = 0$ occurred because the gelation proceeds in the dilute regime ($c_0 < c^*$) with the increase of Ψ^* . After the system reaches the semidilute regime ($c > c^*$),

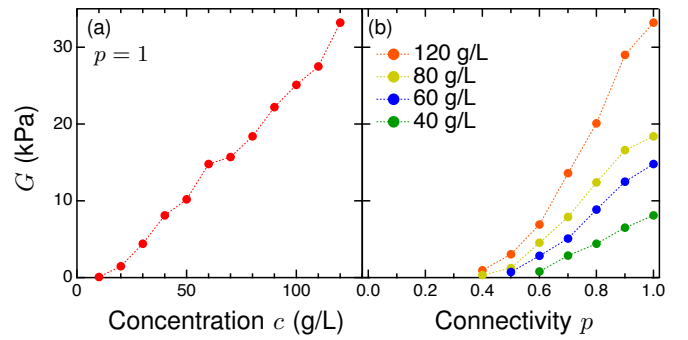


FIG. S5. Shear moduli G of gel samples with a molar mass of precursors $M = 10 \text{ kg/mol}$. (a) Dependence of G on the polymer concentration c at a constant connectivity $p = 1$. We used this data to determine the c -dependence of Π_{mix} shown in the main panel of Fig. 4(a). (b) Dependence of G on connectivity ($p = 2s = 0.4, 0.5, 0.6, 0.7, 0.8, 0.9, 1$) for the various polymer concentrations ($c = 40, 60, 80, 120 \text{ g/L}$). We used this data to determine the p -dependence of Π_{mix} shown in the inset of Fig. 4(a).

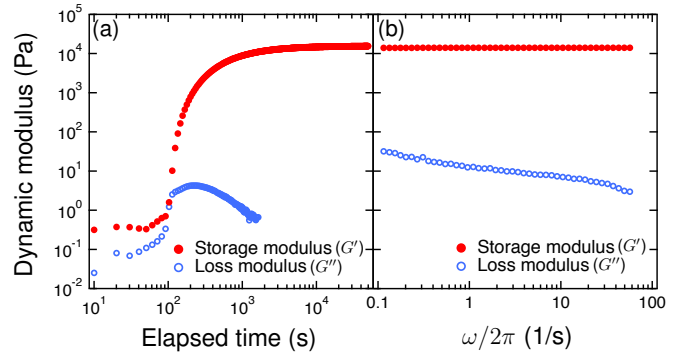


FIG. S6. Storage modulus G' and loss modulus G'' measured by dynamic shear rheometer at 298 K. The sample was prepared with the molar mass of precursors $M = 10 \text{ kg/mol}$, the concentration $c = 70 \text{ g/L}$, and the connectivity $p = 1$. (a) Time courses of G' and G'' during the chemical reaction of the cross-end coupling. Here, the applied strain and frequency are 1% and 1 Hz, respectively. (b) Frequency dependences of G' and G'' after completion of the chemical reaction ($t \gg t_{\text{gel}}$).

the scaling law of Eq. (S5) holds with a constant Ψ^* as p increases.

To evaluate $\hat{\Pi}/\hat{c}^{1.31}$ in Fig. 4(b) in the main text, we substituted $M c^{*1/(3\nu-1)} = 1600 \text{ (kg/mol)(g/L)}^{1/(3\nu-1)}$ into Eqs. (3) and (4) throughout the gelation process for $c_0 = 40, 60, 80, 120 \text{ g/L}$. Here, we assumed that $M c^{*1/(3\nu-1)}$ is constant during the gelation process in the semidilute regime. This is because Π and Π_{mix} are constant in the semidilute regime (see orange squares for $c_0 = 120 \text{ g/L}$ in the inset of Fig. 4(a) in the main text) and the other parameters (R , T , c , and $K \simeq 1.1$) are also constant in Eqs. (3) and (4) in the main text.

S7. MEASUREMENT OF SHEAR MODULUS

To determine Π_{mix} shown in Fig. 4(a) in the main text, we measured the dependences of the shear moduli G of gel samples on the concentration c (Fig. S5(a)) and connectivity p (Fig. S5(b)) by using dynamic viscoelasticity measurements. We mixed the tetra-PEG MA and tetra-PEG SH aqueous solutions and poured the resulting solutions into the gap of the double cylinder of the dynamic shear rheometer (MCR 301 and 302, Anton Paar, Graz, Austria). Then, we cyclically sheared the samples in the gap between the inner cylinder and outer cup. The stress-strain response yields the storage moduli G' and

the loss moduli G'' of the samples.

Figure S6(a) shows the typical time course of G' and G'' . After G' reached equilibrium, corresponding to the completion of the chemical reaction of the MA and SH functional groups, we measured the frequency dependence of G' and G'' (Fig. S6(b)). The (static) shear modulus is given by

$$G = \lim_{\omega \rightarrow 0} G'(\omega). \quad (\text{S6})$$

Figure S6(b) shows that $G'(\omega)$ is independent of the frequency ($\omega/2\pi$) below 100 Hz. Thus, we regard $G'(\omega)$ at 1 Hz as the shear modulus G .

[S1] P. G. de Gennes, *Scaling Concepts in Polymer Physics* (Cornell University Press, Ithaca, 1979).
 [S2] I. Noda, N. Kato, T. Kitano, and M. Nagasawa, *Macromolecules* **14**, 668 (1981).
 [S3] Y. Higo, N. Ueno, and I. Noda, *Polym. J.* **15**, 367 (1983).
 [S4] H. Vink, *Eur. Polym. J.* **7**, 1411 (1971).
 [S5] P. J. Flory, *Principles of Polymer Chemistry* (Cornell University Press, Ithaca, 1953).
 [S6] N. F. Carnahan, and K. E. Starling, *J. Chem. Phys.* **51**, 635 (1969).